

Muscle-driven motion simulation based on deformable human model constructed from real anatomical slice data

Hiroshi INABA, Shin-ya MIYAZAKI, and Jun-ichi HASEGAWA

Graduate School of Computer and Cognitive Sciences, Chukyo University
101 Tokodachi, Kaizu-cho, Toyota-city, Aichi, 470-0393 Japan.
Tel. +81-565-45-0971(ext.6781), Fax. +81-565-46-1299
{inaba, miyazaki, hasegawa}@sccs.chukyo-u.ac.jp

1 Introduction

Recently, many researches have been reported for the purpose of human motion simulation which is applicable to sports medicine, rehabilitation, plastic surgery and so on. Digital human body is a general term for those synthesized models and is expected to analyze and evaluate real human's behaviors. It enables us to experiment many cases safely without giving patients any pain. However, for the time being, those models do not have enough capability to be applied to the practical use.

Not only deformed shapes but also motion features are often important for practical use. Therefore, the model has to be dynamic, motion should be driven by muscle force, and the deformed shape should be decided as a result of elastic object's interaction.

Several kinds of digital human body projects have been reported. [1–3] have developed motion generation driven by muscle force though the model is simplified one because they are in the field of physiology. [4, 5] have constructed human body based on motion capture devices, in which motion is given beforehand, and their purpose is to obtain deformed shape rather than motion generation.

In this paper, we propose a digital human model which is constructed from anatomical slice data and driven by muscle force. The model is composed of rigid bones and deformable tissues such as skeletal muscle and fatty tissue, which generates both motion and deformation of the human body at the same time. In the simulation process, contraction forces are given first to some skeletal muscles in the model, and then corresponding bones are moved. In the next moment, the muscles are not only moved themselves but also deformed due to changes of relative positions of bones. At this time, fatty tissues connected with muscles on the model are also moved and deformed. By iterating the above process at short time intervals, a body motion with shape deformation can be generated. In the experiment, the proposed method is applied to motion simulation of the lower limbs and the results are visualized as animation.

The remaining part of this paper is structured as follows: Section 2 explains the procedure of human body construction from Visible Human anatomical slice

data. Sections 3 and 4 show motion generation and tissue deformation, respectively. In section 5, shows the appropriateness of synthesized deformation is discussed with experimental results. Section 6 shows some conclusions.

2 Human Body Model

2.1 Basic Structure

Our digital human body consists of three components: bone, muscle and fatty tissue. The bone builds a base of posture. The muscle moves the skeleton by contracting itself and constructs an inner shape of human body. The fatty tissue forms a body surface with being deformed by movement of skeleton and deformation of muscle. While each bone is a rigid object, each muscle and fatty tissue are elastic objects.

2.2 Model Components and Construction

The shape of each component is represented as a 3D lattice. It can be constructed by using slice images obtained from a real human body. The detail procedure for construction is as follows. If two or more regions of the same component are included in a slice, the procedure is applied to each of them.

Reduction of number of slices (Fig. 1(a))

Polygonal representation After a border of each component region is extracted from each slice. To do it, a set of intersection points of the border and several lines outgoing radically from the center point of the region is obtained (Fig. 1(b)). These points are vertices of the polygon and a set of lines between two adjoining points is the simplified border (Fig. 1(c)).

3D Construction A 3D shape is constructed by connecting every pair of corresponding vertices between two adjoining slices.

Only the inner surface of the fatty tissue is decided by utilizing the shapes of the bone and muscles (Fig. 2(a)). The detail procedure is as follows.

Reference point selection The center point of the major bone region in each slice is used as the reference point.

Setting of inner points Using lines outgoing radically from the reference point, the following points are obtained:

- Intersection points of the bone border and the radial lines
- Intersection points of the muscle border and the radial lines

These points are regarded as vertices of polygon representing the inner surface of the fatty tissue (Fig. 2(b)). If there exist two points or more on a single radical line, only the nearest one to the reference point is remained and others are omitted (Fig. 2(c)).

3D Construction A 3D lattice is constructed the same way for other components mentioned above.

The whole shape of the fatty tissue is obtained as shown in Fig. 2(d) by combining the inner surface as in Fig. 2(c) and the other as in Fig. 1(c). An example of constructed body components is shown as Fig. 3.

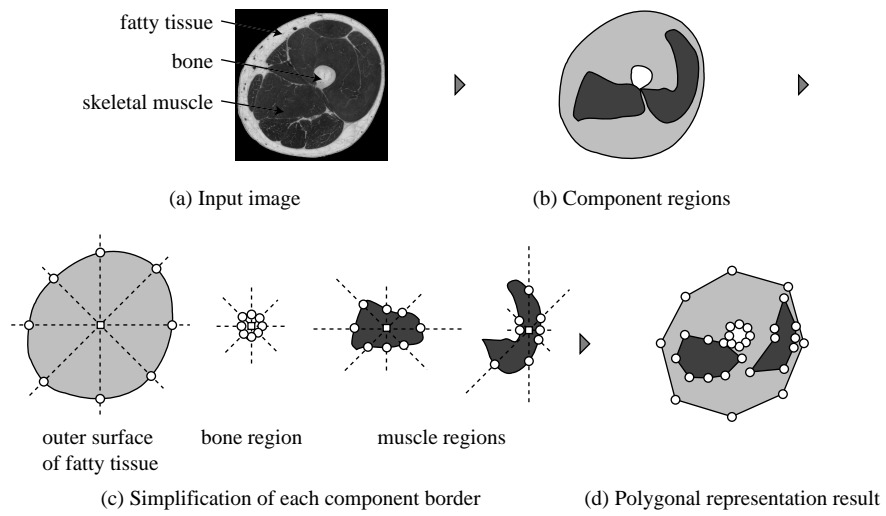


Fig. 1. Construction of components

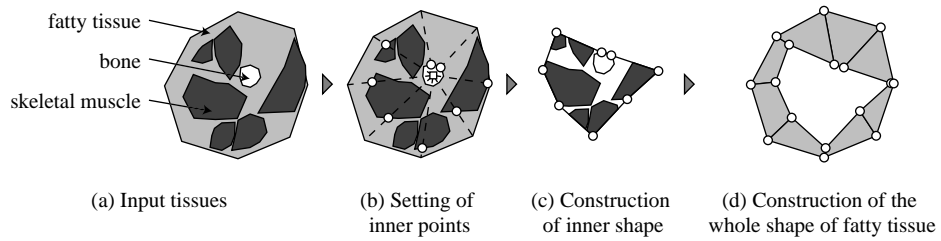


Fig. 2. Construction of fatty tissue shape

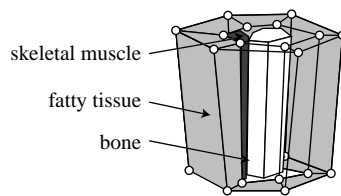


Fig. 3. An example of constructed body parts

3 Motion Generation

3.1 Outline of Motion Generation

Each muscle can generate a force for contracting itself. This force is transformed to a joint torque to rotate and move the skeleton connected to the muscle. Shapes of muscle and fatty tissue are deformed according to the postural change of the skeleton. By performing this process repeatedly, a human motion is generated. The results are visualized in the form of animation (Fig. 4).

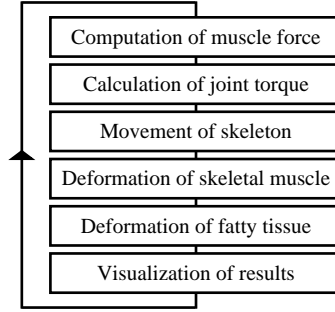


Fig. 4. Procedures of motion generation

3.2 Muscle Contraction

An active human motion is basically generated by muscle contraction. An extra force for constructing a muscle is called “contraction force”, and is applied to each of specified muscles. This force has a part for shortening muscle length.

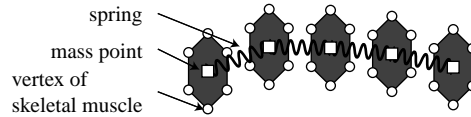


Fig. 5. Arrangement of mass points and springs

Fig. 5 shows an example of mass points and springs arrangement. Some mass points and springs connected in series are placed on the center axis of muscle. The contraction force \mathbf{F}_i applied to mass point i is given by Eq. (1). m_i , i , k , L , and D represent a mass of point, spring constant, natural length of spring, and experimentally with considering damper, respectively. \mathbf{r}_{ij} is a relative vector from point i to point j , and \mathbf{v}_{ij} is the relative velocity from point i to point j .

A configuration of mass points is determined under the effect of the contraction force. A muscle is attached to a skeleton only through a mass point, called muscle end point, paced on the muscle end. So, only the force on the muscle end point operates to the skeleton directly. Therefore, using the force on and the position of the muscle end point can calculate a joint torque.

$$\mathbf{F}_i = m_i \cdot \mathbf{g} \sum_j \left\{ k \cdot \left(1 - \frac{L}{|\mathbf{r}_{ij}|} \right) \cdot \mathbf{r}_{ij} + D \cdot \mathbf{v}_{ij} + M \cdot \frac{L}{|\mathbf{r}_{ij}|} \right\} \quad (1)$$

4 Tissue Deformation

4.1 Muscle deformation

Skeletal muscles are deformed according to the movement of the skeleton. The deformation is performed based on a movement of mass points arranged on a centerline of skeletal muscle. The detail procedure is as follows.

Restriction of constant volume The whole shape of each muscle is deformed to keep its volume constant. This is based on the reason that the real muscle's volume is almost unchanged even if it deforms strongly. Along with muscle is getting shrinked, sectional areas of the muscle increase contrastly Fig. 7).

Restriction of mass point movement To restrict the area of mass point movement, mass points are anchored onto the bone surface. At first the closest polygon to each mass point is searched. Then, the center of gravity of the polygon is decided as anchor point. Mass point movement is restricted in a conic region located according to the anchor point as shown in Fig. 6). The top of the cone corresponds to the anchor point and the medial axis goes through the anchor point and the mass point in the initial state.

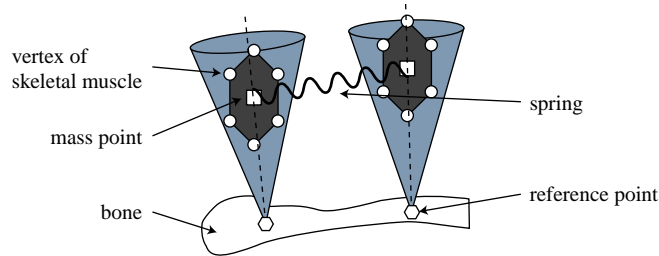


Fig. 6. Conic areas for restricting mass point movement

4.2 Fatty tissue deformation

Elastic model of fatty tissue To obtain a deformed shape of fatty tissue, an elastic object model developed by our group [6] is employed. In this model, the

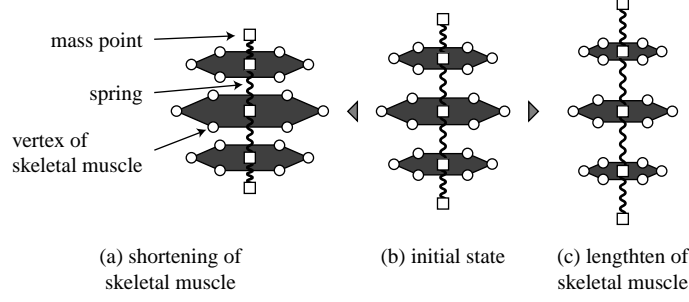


Fig. 7. Illustration of skeletal muscle deformation

whole shape is represented by a set of volume elements. Each volume element should be a polyhedron. This model generates proper stress for restoring the initial shape even if the object extremely deforms. It has a feature that a 3D structure of the local shapes in comparison with an ordinary mass-and-spring model. The elastic calculation in this model is faster than in the mass-and-spring model. Also, an elastic object based on this model is more robust for large-scale deformation than that by the mass-and-spring model.

Displacements of mass points in each local element are obtained as $\mathbf{r}_i - \mathbf{R}_i$ to satisfy the Eq. 2. Here \mathbf{R}_i shows the relative vector of the vertex i in the equilibrium shape with respect to the gravity of the element. Also \mathbf{r}_i shows the relative vector of the vertex i in the deformed shape. k is elastic constant to decide flexibility of deformation. In fact; \mathbf{R}_i is obtained to solve the Eqs. 3,4, where \mathbf{R}_i is the initial position of \mathbf{R}_i . $u = (u_x, u_y, u_z)$ means the unit vector of the rotation axis and θ shows the rotation angle.

$$\sum_i \mathbf{r}_i \times (\mathbf{R}_i - \mathbf{r}_i) = K \sum_i \mathbf{r}_i \times \mathbf{R}_i = \vec{0} \quad (2)$$

$$\mathbf{R}_i = \mathbf{M} \cdot \mathbf{R}_i \quad (3)$$

$$\mathbf{M} = \mathbf{u}\mathbf{u}^T + \cos \theta (\mathbf{I} - \mathbf{u}\mathbf{u}^T) + \sin \theta \begin{pmatrix} 0 & -u_z & u_y \\ u_z & 0 & -u_x \\ -u_y & u_x & 0 \end{pmatrix} \quad (4)$$

Deformation Deformation of the fatty tissue consists of the global deformation by a change of posture and local deformation by a change of muscle shape. The detail procedure is as follows (Fig. 8).

A reference points As shown in Fig. 8(a), for a vertex p of fatty tissue selection facing the skeletal muscle, the closest vertex g of the skeletal muscle is selected. g is called the reference point of p .

Acquirement of moving vector When a shape of the skeletal muscle is defined by a change of posture. The movement of each vertex is represented by a moving vector (Fig. 8(b)).

Deformation of inner shape of fatty tissue If a vertex of the skeletal muscle is a reference point, and its moving vector is \mathbf{v} , the corresponding vector of the fatty tissue is also moved by \mathbf{v} (Fig. 8(c)).

Deformation of whole shape of body surface After the above process, the shape of each volume element is changed based on the elastic calculation. This results in the deformation of the whole shape of fatty tissue. This also means that a body surface (+ the outer shape of fatty tissue) is obtained (Fig. 8(d)).

If a vertex that is arranged to the inside of fatty tissue touches a bone, it is only moved on the bone and the above process is not performed.

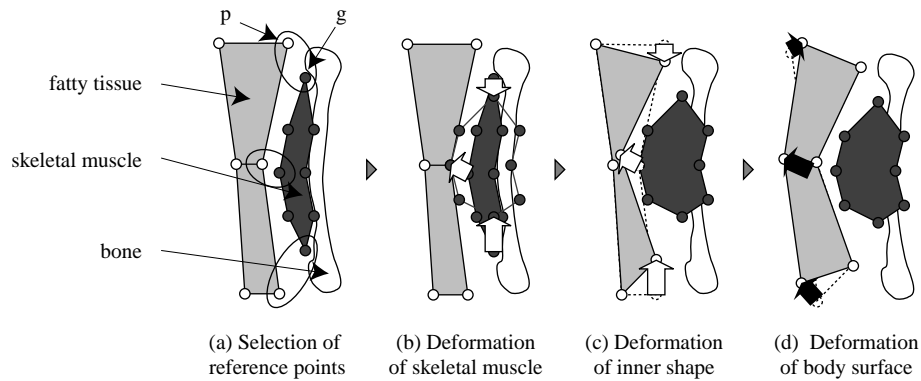


Fig. 8. Illustration of fatty tissue deformation

5 Experiments and Discussion

5.1 Experiments

Outline of muscle behaviors In following experiments, our model is applied to a human leg. A flexion motion at a knee joint is generated. A model of the lower limb is composed of 16 muscles. Some muscles have a roll to generate a flexion motion, others simply deforms depending on them and form the outline around the pelvis.

Construction of human body model We extracted the shape of bone, muscle and fatty tissue from axial photographs of the Visible Human Dataset [8] (slice no. 1700-2878). Table 1 shows a specification of original images and input

images. We used clipping images to calculate an elastic equation quickly and selected images at intervals of 5 slices to obtain a rough shape of tissues. Each tissue component is extracted by semiautomatically. The model is simplified in resolution for fast computation, and the degree of simplification is decided by comparing the resultant shape with the original one. As a result, the number of polygon in the constructed model is about 0.5 percent compared with the model constructed by using ordinal Marching cubes method. In our current model, the knee joint has a mechanism to rotate around an identical point and it has limits in rotation angle. For the mass and the moment of inertia of bone, we used the parameter values in ref. [7].

The final results are visualized as a 3D animation. We can see the behavior of both bone and muscle transparently.

Table 1. Specification of images

	<i>Original image Input image</i>	
image size(pixel)	2048×1216	290×337
pixel size(mm)	0.33×0.33	1×1
number of images	1179	236
image interval(mm)	1	5

5.2 Results

Fig. 9-11 show experimental results. Fig. 9 shows the results of motion simulation for the lower limbs. In the figures, deformed body surfaces at a knee joint can be observed in motion. Fig. 10 and Fig. 11 show the knee joint part and the femur part, respectively, in the same simulation, In these figures, fatty tissue deformation and muscle deformation are demonstrated well. We realized real-time processing for generation of human motion by using a standard PC (Spec; Pentium III 1GHz×2, 1GB Memory, GeForce3, OS; Windows 2000).

5.3 Discussion

Motion Generation From the experimental results, it is confirmed that a flexion motion at a knee joint can be generated by contractions of skeletal muscles arranged at the femur. Although in this paper, we presented only simulation results for a single motion, our method can generate various motions by modifying the timing and parameters of muscle contraction. However, the property of contraction force used in our skeletal muscle model is different from that of real human because of employing a single model based on the behavior of spring for skeletal muscles. Also, our skeletal muscle cannot generate any motion based on cooperative works by plural muscles. To solve this problem, a biomechanics

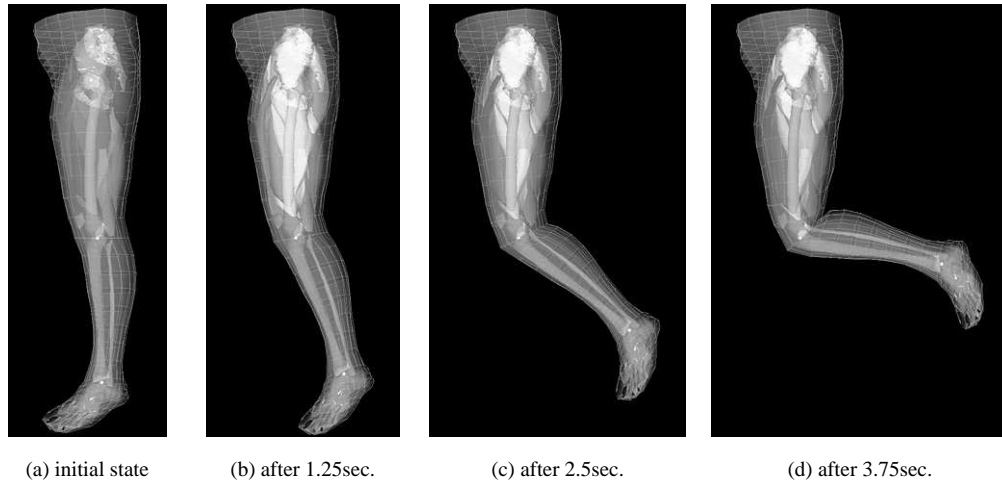


Fig. 9. Results of motion generation

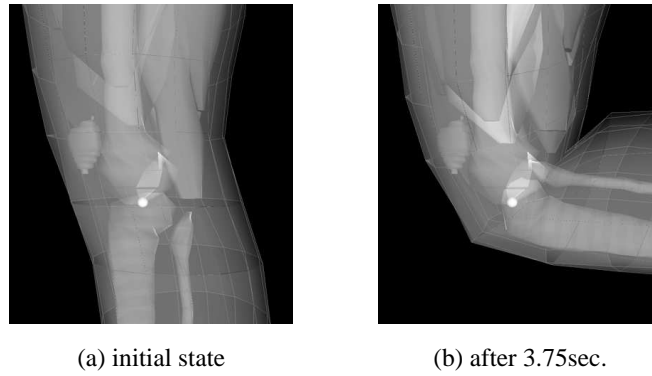


Fig. 10. A result of body surface deformation at a knee joint

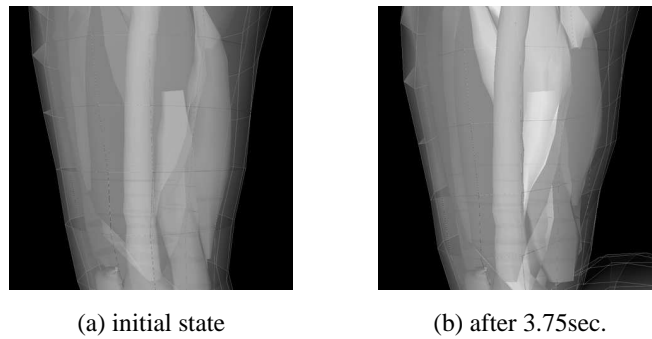
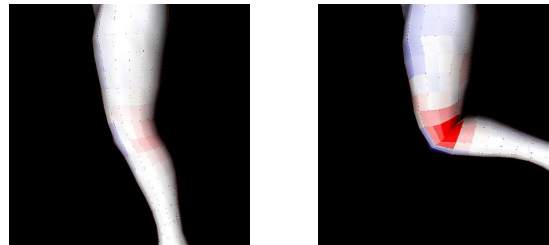


Fig. 11. A result of tissue deformation of the femur

model of skeletal muscle must be introduced (e.g. ref. [9]). If such a higher performance model is realized, it will become possible to generate more complicated and continuous motion, such as a stand-up motion and kick motion.

Tissue deformation In the experiments deformation of the whole shape of the lower limbs in motion can be observed. Especially, in the knee joint part, the shape of the fatty tissue is subject to change greatly. The result of body surface deformation at the front of the knee joint was very natural, but at the back of the knee joint, the result had some heavy caves to the inside of the human body. This tendency was confirmed independent of the degree of body shape simplification was changed. Also, unexpected phenomena were found that the shape of fatty tissue was broken when the degree of deformation became heavy or the joint angle became too large. The main reason is a failure of elastic calculation due to heavy deformation.

Visualization of results For a motion simulation system with deformable body model proposed here, it is very important and useful to develop a function for visualizing the deformation results in detail. Therefore, the degree of deformation is visualized by classifying them with colors. Fig. 12 shows a change of the body surface area from the initial state to the current state in a motion. The area of body surface part for each volume element of fatty tissue is measured, and a color is assigned to each part of the current surface according to the difference between areas of the initial and the current states. In Fig. 12, white color means no difference, and blue and red mean increase and decrease of deformation, respectively,



(a) after 1.25sec.

(b) after 3.75sec.

Fig. 12. Visualization of change of body surface area

Fig. 13 shows a change of fatty tissue shape from the initial state to the current state. The degree of fatty tissue deformation for each volume element of fatty tissue is calculated by Eq. (5). $\mathbf{R}\mathbf{o}_i$ and \mathbf{r}_i are the same as defined by Eq.

2. N is the number of vertices in a fatty tissue volume element.

$$\frac{\sum_{i=1}^N |\mathbf{R}\mathbf{o}_i - \mathbf{r}_i|}{N} \quad (5)$$



Fig. 13. Visualization of change of fatty tissue shape

The colors are assigned in the same manner as mentioned above.

These visualization results make it easy to understand a change of the tissue shape in a special situation such as a loss of tissue function and a change of the internal structure of human body. Also these can be used for giving an informed consent in medical field, especially cosmetic surgery.

6 Conclusions

In this paper, a digital human model with movable and deformable body was proposed. This model consists of skeleton, muscle and fatty tissue, and can be used for motion generation with body shape deformation. In experiments, the model was applied to the motion generation of human lower limbs. The results are promising. Our future works include evaluation of the reality for motion and shape generated by our model, generation based on cooperative works by plural muscles, muscle deformation based on elasticity of muscle itself, and application to other parts in the human body.

Acknowledgments

The authors thank colleagues of the Hasegawa laboratory for much discussion. This work was supported in part by the grant-in-aid for Private University High-Tech Research Center, Ministry of Education, Culture, Sports, Science and Technology, Japan

References

1. MusculoGraphics Inc.: SIMM (Software for Interactive Musculoskeletal Modeling). <http://www.musclographics.com>
2. Taku KOUMURA, Yoshihisa SHINAGAWA, Toshiyasu L. KUNII: Creating and re-targeting motion by the musculoskeletal human body model. *The Visual Computer* 16:254-270 (2000)
3. Kazunori HASE, Junya NISHIGUCHI, Nobutoshi YAMAZAKI: Model of Human Walking with Three-Dimensional Musculo-Skeletal System and Hierarchical Neuronal System. *Biomechanism 15*, Society of Biomechanisms Japan ,pp.187-198 (June 2000) (in japanese)
4. Kenichi YAMAZAKI, Naoki SUZUKI, Asaki HATTORI, Akihiko TAKAMATSU, Akihiko UCHIYAMA: The Development of 4D Muscle Model for 4D Quantitative Movement Analysis. *Journal of JSCAS*, Vol. 2, No. 1, pp.22-29 (May 2000) (in japanese)
5. Luciana Porcher Nedel, Daniel Thalmann: Anatomic modeling of deformable human bodies. *The Visual Computer* 16:306-321 (2000)
6. Shin-ya MIYAZAKI, Shunsuke YOSHIDA, Takami YASUDA, Shigeki YOKOI: Proposal to Model Elastic Objects Based on Maintaining Local Shapes. *The Transactions of IEICE*, Vol. J82-A, No. 7, pp.1138-1155 (1999) (in japanese)
7. Dempster WT.: Space requirements of the seated operator. WADC Technical Report, Wright-Patterson Air Force Base, pp.55-159 (1955)
8. Michael J. Ackerman: The Visible Human Project. *Proceedings of IEEE*, Vol. 86, No. 3 (March 1998)
9. Felix E.Zajac: Muscle and Tendon: Properties, Models, Scaling, and Application to Biomechanics and Motor Control. *Critical Reviews in Biomedical Engineering*, Vol. 17 Issue 4, (1989)